Preprints of the 19th World Congress
The International Federation of Automatic Control
Cape Town, South Africa. August 24-29, 2014

Energy Based Set Point Modulation for Obstacle Avoidance In Haptic Teleoperation of Aerial Robots

Xiaolei Hou [**,*] **Changbin Yu** [*,**] **Feng Liang** [**] **Zhiyun Lin** [***]

[*] *Shandong Computer Science Center, Jinan, 250014, China*
[**] *Australian National University, Canberra, ACT 0200, Australia*
[***] *College of Electrical Engineering and State Key Laboratory of Industrial Control Technology, Zhejiang University, Hangzhou, 310027, China*
(e-mail: {xiaolei.hou, brad.yu}@anu.edu.au, liangf@sdas.org, linz@zju.edu.cn)

Abstract: This paper presents a novel obstacle avoidance approach that is capable of dealing with both static and dynamic obstacles in the environment with guaranteed collision-free navigation for haptic teleoperation of VTOL aerial robots. The proposed approach modulates the set point for the vehicle's controller based on the user input energy, estimated potential energy and vehicle's kinetic energy. By shuffling the potential and kinetic energy, vehicle's velocity is regulated according to the permissible kinetic energy and thus obstacle avoidance is achieved. With careful design of the potential field, this approach offers a guaranteed collision-free navigation with the presence of both stationary and moving obstacles. Incorporating the novel approach with the *Dynamic Kinesthetic Boundary*, the human operator can better perceive the environment where the robot is deployed through the rich spatial haptic cues rather than an onset gradual single force vector. Analysis is provided and proves that in the case of perfect velocity tracking of the slave system, the proposed algorithm can guarantee a collision-free navigation through the environment. Simulations and experiments were conducted, and the results provide verification of the effectiveness of the proposed approach in obstacle and collision avoidance for haptic teleoperation of aerial robots.

Keywords: Obstacle avoidance; Teleoperation; Robotics

1. INTRODUCTION

Haptic feedback was first introduced into teleoperation of mobile robots to improve the human operator's performance in safely navigating vehicle through complex remote environment(Hong et al. [1999]), and its effectiveness has been proved in previous works (Diolaiti and Melchiorri [2002], Lee et al. [2002], Brandt and Colton [2010], Lam et al. [2009], Mahony et al. [2009], Hou et al. [2013]). Most of these works adopt viscous-elastic coupling between slave robots and environment for generating an exogenous force that is derived from the collected sensor data to provide the user with perception of the potential dangers in the environment.

Potential field is one of the most common approaches for mobile robot's obstacle avoidance and navigation by generating repulsive or attractive forces. A *Generalized Potential Field* is proposed (Krogh [1984]) to deal with the infinite force when the distance decreases to zero by including velocity and deceleration information. A series of works (Boschloo et al. [2004], Lam et al. [2007, 2009]) compare the performances of different obstacle avoidance approaches, including *Generalized Potential Field* (GPF), *Basic Risk Field* (BRF) and *Parametric Risk Field* (PRF). Schill et al. [2008] and Mahony et al. [2009] investigated the optical flow based obstacle avoidance approach. In Brandt and Colton [2010], comparisons among various obstacle avoidance approaches were conducted again. All aforementioned works came to a similar conclusion that, obstacle avoidance algorithms including a velocity-over-distance term would generally have better performance than the others. The Time-To-Impact (TTI) approach in Brandt and Colton [2010] appears identical to the optical flow formula that is velocity-over-distance.

In addition to the force feedback in previous works that provide a gradual onset force vector that combines both environmental forces and vehicle's dynamic forces(Mersha et al. [2012]), spatial haptic cues were also investigated that offer the user with distinguishing and rich haptic information of the remote environment. Kim et al. [2006] investigated rendering spatial cues for aiding the operator

⋆ This work was supported in part by the Australian Research Council through Discovery Project DP-130103610, a Queen Elizabeth II Fellowship under Grant DP110100538 and Overseas Expert Program of Shandong Province, and a grant from Shandong Academy of Science Development Fund for Science and Technology, and the Pilot Project for Science and Technology in Shandong Academy of Science, the Open Research Project of the State Key Laboratory of Industrial Control Technology, Zhejiang University (No. ICT1427), Zhejiang Provincial Natural Science Foundation of China LR13F030002, and the National Natural Science Foundation of China (61375072).

to perceive the environment and avoid collisions in manipulator teleoperation. The *Restriction Space Projection* (RSP) provides human operator with the perception of the *Instantaneous Restriction Space* (IRS), the configuration space that the manipulator can not reach either due to the obstacles or the geometric constraints. For mobile robot teleoperation, Hou and Mahony [2013] introduced *Dynamic Kinesthetic Boundary* (DKB) that maps the remote environment information to spatial haptic cues in joystick's workspace and modulates the velocity reference to vehicle's controller in accordance with this spatial information to achieve obstacle avoidance. A similar approach presented by Omari et al. [2013] also exploits the spatial cues for perceiving environment and obstacle avoidance.

In this paper, we propose an energy based set point modulation for obstacle avoidance in haptic teleoperation of VTOL aerial robots under passive teleoperation framework, which is inspired by the Passive-Set-Point-Modulation approach Lee and Huang [2010] that deals with variable time delay in communication. The proposed approach invokes the passive teleoperation framework incorporating the explicitly defined potential energy to achieve collision-free guaranteed performance by modulating vehicle's velocity set point with respect to the permissible kinetic energy. The novel approach integrates the potential energy into the system as part of the vehicle's energy, which is always charged or discharged first and instantaneously and bounded by a ceiling maximum energy that a vehicle can store. A user desired energy is assessed by the raw velocity set point input from user, then compared with the excessive potential energy that overflows the potential energy tank or the permissible kinetic energy, the remaining user input energy, for modulating the velocity set point to the slave vehicle. The passivity of the teleoperation system can be easily preserved with a proper potential energy estimation and energy ceiling, i.e. bounded potential energy. Lemmas are provided and approve that, in the case of perfect velocity tracking, the slave robot can avoid collisions in the environment with both static obstacles and dynamic obstacles moving slower than vehicle's maximum velocity. Moreover, this approach can also be incorporated with the DKB to offer pilot with better perception of the environment. Simulations and experiments were conducted, outcomes of which demonstrate the performance of the proposed approach.

The rest part of the paper is organized as follows. Sect. 2 describes the proposed approach in details. In Sect. 3, the analysis provides theoretical proof of the proposed approach's performance. The implementation of the proposed approach in dynamic kinesthetic boundary is presented in Sect. 4. Sect. 5 provides the results of simulation and experiments. Conclusion is given in Sect. 6.

2. ENERGY BASED OBSTACLE AVOIDANCE

Consider a passive teleoperation system framework for mobile robots (Lee et al. [2006], Stramigioli et al. [2010], Zuo and Lee [2010]), the user input energy is used to drive the slave system and stored in the slave system as kinetic energy or dissipated through damping injection or environmental port. In this section, we introduce the potential energy into the passive system framework as part of the slave system properties, the same as the kinetic energy. Definitions of other energies in the system are also provided and the proposed energy based obstacle avoidance approach is presented in the sequel.

2.1 Coordination System

Given a spherical coordination system in the slave's body fixed frame (BFF) represented by radial distance λ, azimuth θ and elevation ϕ, let $\eta(\theta,\phi,t) \in \mathbf{S}^2$ denote the unit directional vector along the angle pair(θ,ϕ),

$$\eta(\theta,\phi) = \begin{pmatrix} \cos(\theta)\cos(\phi) \\ \sin(\theta)\cos(\phi) \\ \sin(\phi) \end{pmatrix} \in S^2. \tag{1}$$

$\lambda(\theta,\phi,t)$ denotes the radial distance from the slave robot to the obstacle in the bearing direction $\eta(\theta,\phi)$ at time t in the BFF.

2.2 System Energy

Potential Energy The potential energy is designed based on the environment potential field and assessed at the current location of the robot. To achieve good performance of obstacle avoidance and avoid violation of the system passivity, the potential energies of both environment and slave system have to be bounded. Hence, we propose that the potential energy $E_p(\theta,\phi,t) \in \mathbf{R}$ can be estimated by

$$E_{\mathrm{p}} = \frac{1}{2}\left(\frac{2d_{\mathrm{sf}}}{\lambda(\theta,\phi,t)+d_{\mathrm{sf}}}\right)^2 v_{\max}^T M_{\mathrm{s}} v_{\max} \tag{2}$$

where $\lambda(\theta,\phi,t) \in \mathbf{R}$ and $d_{\mathrm{sf}} \in \mathbf{R}$ denote the current distance measurement in the bearing of $\eta(\theta,\phi) \in \mathbf{S}^2$ and the safety distance to the obstacle, $v_{\max} \in \mathbf{R}^3$ is the maximum velocity of the vehicle, and M_{s} denotes the inertia matrix of the vehicle.

The potential energy that vehicle can store is bounded by a ceiling $E_{\max}$

$$E_{\max} = \frac{1}{2} v_{\max}^T M_{\mathrm{s}} v_{\max}, \tag{3}$$

while from (2), we can observe that the maximum estimated potential energy is $2v_{\max}^T M_{\mathrm{s}} v_{\max}$, $\lambda(\theta,\phi,t) \to 0$; and when slave reaches the safety distance d_{sf}, the potential energy reaches the ceiling, i.e. $E_{\mathrm{p}} = \frac{1}{2} v_{\max}^T M_{\mathrm{s}} v_{\max}$.

Note that the potential energy has the following three properties:

- The potential energy is always first charged to the corresponding level at current location instantaneously;
- If there exists excessive potential energy, the excessive potential energy will be discharged by using this energy to drive the slave away along the potential field's greatest gradient direction at the supply rate of $-|u^T v|$, where $u \in \mathbf{R}^3$ is the control output of slave's velocity controller and $v \in \mathbf{R}^3$ is the robot's velocity;
- If user input energy is inadequate to supply the slave's potential energy, the vehicle's kinetic energy will be drawn to supply the potential energy.

Vehicle Total Energy Vehicle total energy is the energy that the slave robot can store and is bounded by an upper bound $E_{\max}$ in (3), that is also the maximum potential energy and maximum kinetic energy of the slave.

User Desired Kinetic Energy Given the user velocity reference input, the user desired kinetic energy E_{d} is an estimate of the vehicle's kinetic energy in the case that the slave system servos the set point $v_{\mathrm{ref}} \in \mathbf{R}^3$ and reaches a new level of kinetic energy,

$$E_{\mathrm{d}} = \frac{1}{2} v_{\mathrm{ref}}^T M_{\mathrm{s}} v_{\mathrm{ref}}. \tag{4}$$

Permissible Kinetic Energy Given the bounds on the vehicle total energy $E_{\max}$ and the potential energy stored in the slave system E_{p}, the permissible kinetic energy $\hat{E}_{\mathrm{k}}$ is the maximum kinetic energy that the robot can achieve at current location, and can be represented as

$$\hat{E}_k = |E_{\max} - E_{\mathrm{p}}| \tag{5}$$

Note that even if user desires more kinetic energy by giving a large velocity set point, the slave vehicle can not achieve the user velocity reference input due to the bounds on the permissible kinetic energy, and hence the obstacle avoidance is implemented in the sense of the monotonic decreasing on the maximum achievable velocity as the vehicle approaches the obstacles.

Considering the possibility of excessive potential energy in the system when the vehicle passes the safety distance d_{sf}, i.e. $E_{\max} - E_{\mathrm{p}} < 0$, the excessive potential energy is assign as the permissible kinetic energy to drive the slave robot away from obstacle for discharging. Given the permissible kinetic energy $\hat{E}_{\mathrm{k}}$ for the vehicle, the modulated velocity set point $v^*_{\mathrm{ref}} \in \mathbf{R}^3$ can be derived as

$$v^*_{\mathrm{ref}} = \begin{cases} \sqrt{\frac{2}{m}\min(\hat{E}_{\mathrm{k}}, E_{\mathrm{d}})}\frac{v_{\mathrm{ref}}}{\|v_{\mathrm{ref}}\|}, & \text{if } E_{\mathrm{p}} \le E_{\max} \\ -\sqrt{\frac{2}{m}(E_{\mathrm{p}} - E_{\max})}\frac{v_{\mathrm{ref}}}{\|v_{\mathrm{ref}}\|}, & \text{if } E_{\mathrm{p}} > E_{\max} \end{cases} \tag{6}$$

where m denotes the mass of the slave system.

2.3 System Architecture

To incorporate the potential energy with the passive teleoperation system framework, an energy supervisor is provided to estimate and charge/discharge the potential energy at different locations, and modulate the velocity reference according the permissible kinetic energy. The implementation of proposed approach in a teleoperation system is shown in Fig. 1 and the complete energy based obstacle avoidance algorithm is described in Alg. 1.

Algorithm 1. Energy Based Obstacle Avoidance

$E_{\max} \Leftarrow \frac{1}{2} v_{\max}^T M_{\mathrm{s}} v_{\max}$, $E_{\mathrm{p}}(0) \Leftarrow 0$, $\hat{E}_{\mathrm{k}}(0) \Leftarrow 0$
repeat
  estimate $E_{\mathrm{p}}(t)$
  if $v_{\mathrm{ref}}(t)$ is received **then**
    compute $E_{\mathrm{d}}(t)$
    if $E_{\mathrm{p}}(t) \le E_{\max}$ **then**
      $v^*_{\mathrm{ref}}(t) = \sqrt{\frac{2}{m}\min_{v^*_{\mathrm{ref}}(t)}(\hat{E}_{\mathrm{k}}(t), E_{\mathrm{d}}(t))}$
      send $v^*_{\mathrm{ref}}(t)$ to vehicle's velocity controller
    else
      find $v^*_{\mathrm{ref}}(t)$ by solving $-\sqrt{\frac{2}{m}(E_{\mathrm{p}}(t) - E_{\max})}$
    end if
  end if
until termination

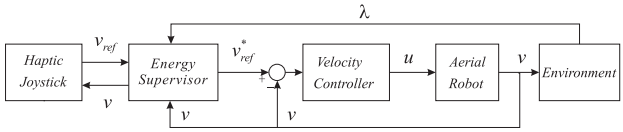

Fig. 1. System architecture.

3. ANALYSIS

In this section, we first provide system passivity analysis and then present two lemmas to prove that, the proposed energy based obstacle avoidance approach is capable of assisting the operator to safely navigate the slave robot through the environment with both static and dynamic obstacles.

3.1 System Passivity

Given the human operator is passive, both master joystick and slave robot are passive, the stable passive teleoperation system framework for mobile robots as in Zuo and Lee [2010] or Lee et al. [2006] can be achieved in the sense that: $\forall T$,

$$\begin{aligned} \int_0^T (f_{\mathrm{m}}^T \dot{\xi} + f_{\mathrm{s}}^T v_{\mathrm{s}}) dt \\ &= V_{\mathrm{m}}(T) - V_{\mathrm{m}}(0) + V_{\mathrm{s}}(T) - V_{\mathrm{s}}(0) \\ &\ge -V_{\mathrm{m}}(0) - V_{\mathrm{s}}(0) \end{aligned} \tag{7}$$

where $f_{\mathrm{m}} \in \mathbf{R}^3$ and $\dot{\xi} \in \mathbf{R}^3$ denote the force and velocity of the master joystick, M_{m} and M_{s} are the inertial matrix of master and slave device. $V_{\mathrm{m}}(t) := \frac{1}{2}\dot{\xi}^T M_{\mathrm{m}} \dot{\xi}$ and $V_{\mathrm{s}}(t) := \frac{1}{2} v_{\mathrm{s}}^T M_{\mathrm{s}} v_{\mathrm{s}}$ are the energy of the master and the slave system at time t.

Provided the potential energy in (2), the supply rate of the potential energy can be derived as

$$\frac{4 d_{\mathrm{sf}} v_{\max}^T M_{\mathrm{s}} v_{\max}}{(\lambda + d_{\mathrm{sf}})^3} \|v_{\mathrm{s}}\|, \tag{8}$$

which is bounded by

$$\frac{4 v_{\max}^T M_{\mathrm{s}} v_{\max}}{d_{\mathrm{sf}}^2} \|v_{\max}\|, \tag{9}$$

such that $\forall$ T,

$$\int_0^T \frac{4 d_{\mathrm{sf}} v_{\max}^T M_{\mathrm{s}} v_{\max}}{(\lambda + d_{\mathrm{sf}})^3} \|v_{\mathrm{s}}\| dt = E_{\mathrm{p}}(T) - E_{\mathrm{p}}(0) \ge -E_{\mathrm{p}}(0) \tag{10}$$

and system's two-port passivity can be obtained: $\forall$ T,

$$\begin{aligned} \int_0^T (f_{\mathrm{m}}^T \dot{\xi} + f_{\mathrm{s}}^T v_{\mathrm{s}} + \frac{4 d_{\mathrm{sf}} v_{\max}^T M_{\mathrm{s}} v_{\max}}{(\lambda + d_{\mathrm{sf}})^3} v_{\mathrm{s}}) dt \\ &= V_{\mathrm{m}}(T) - V_{\mathrm{m}}(0) + V_{\mathrm{s}}(T) - V_{\mathrm{s}}(0) + E_{\mathrm{p}}(T) - E_{\mathrm{p}}(0) \\ &\ge -V_{\mathrm{m}}(0) - V_{\mathrm{s}}(0) - E_{\mathrm{p}}(0) \end{aligned} \tag{11}$$

Therefore, if the passive teleoperation system is stable, the new system integrated with the proposed obstacle avoidance algorithm will still be passive and stable.

3.2 Obstacle Avoidance Performance

Lemma 1. Assume that the slave robot is moving in a locally smooth static environment with bounded curvature.

Given perfect velocity tracking performance $v = v^*_{\text{ref}} \in \mathbf{R}^3$, the proposed approach will prevent vehicle's collision with environment, s.t. $\forall t > 0$ and $d_{\text{sf}} > 0$,

$$\lambda(\theta, \phi, t) > 0, . \tag{12}$$

Proof. Define

$$y(t) = \min_{(\theta,\phi)\in\mathbf{S}^2} (\lambda(\theta, \phi, t) + d_{\text{sf}}). \tag{13}$$

Since $\mathbf{S}^2$ is compact, there always exists an azimuth-elevation pair (θ^*, ϕ^*) that realizes (13) by

$$y(t) = \lambda(\theta^*, \phi^*, t) + d_{\text{sf}}. \tag{14}$$

The proof proceeds by contradiction.

Assume $\exists$ a first finite time $t_0 > 0$, such that

$$\lim_{t\to 0} y(t) = d_{\text{sf}}, \tag{15}$$

i.e.

$$\lim_{t\to 0} \lambda(\theta^*, \phi^*, t) = 0. \tag{16}$$

Since the permissible kinetic energy $\hat{E}_{\text{k}}$ in the system is always bounded by $E_{\max} - E_{\text{p}}$, therefore, the velocity of the vehicle is also bounded,

$$\sqrt{\frac{2}{m}(E_{\max} - E_{\text{p}})} \geq \langle v(t), \eta(\theta^*, \phi^*)\rangle \geq -\|v(t)\|. \tag{17}$$

From the upper bound of the velocity in (17) and the permissible kinetic energy in (6), one has the following inequality,

$$\begin{aligned} \langle v(t), \eta(\theta^*(t), \phi^*(t))\rangle^2 &\leq \|v_{\max}\|^2 (1 - \frac{4d_{\text{sf}}^2}{(\lambda(\theta^*, \phi^*, t) + d_{\text{sf}})^2}) \\ \frac{\langle v(t), \eta(\theta^*(t), \phi^*(t))\rangle^2}{\|v_{\max}\|^2} &\leq \frac{(\lambda(\theta^*, \phi^*, t) + d_{\text{sf}})^2 - 4d_{\text{sf}}^2}{(\lambda(\theta^*, \phi^*, t) + d_{\text{sf}})^2} \end{aligned} \tag{18}$$

Let α denote the $\frac{\langle v(t), \eta(\theta^*, \phi^*)\rangle}{\|v_{\max}\|}$, and recall (13), (18) becomes

$$\begin{aligned} \alpha^2 &\leq \frac{y(t)^2 - 4d_{\text{sf}}^2}{y(t)^2} \\ 4d_{\text{sf}}^2 &\leq (1 - \alpha^2) y(t)^2 \end{aligned} \tag{19}$$

Considering the perfect tracking assumption $v = v^*_{\text{ref}}$, and the maximum velocity bound $\|v^*_{\text{ref}}\| \leq \|v_{\max}\|$, one has

$$1 \geq 1 - \alpha^2 \geq 0, \tag{20}$$

and combining (19) and (13), we have

$$\begin{aligned} 4d_{\text{sf}}^2 &\leq y(t)^2 \\ 2d_{\text{sf}} &\leq y(t) \end{aligned}, \tag{21}$$

i.e.

$$\begin{aligned} 2d_{\text{sf}} &\leq \lambda(\theta^*, \phi^*, t) + d_{\text{sf}} \\ d_{\text{sf}} &\leq \lambda(\theta^*, \phi^*, t) \end{aligned}. \tag{22}$$

The inequality (21) and (22) are clearly contradictory to the assumption (15) and (16). Therefore, $\forall t > 0$, $\lim_{t\to 0} y(t) \neq d_{\text{sf}}$ and $\lim_{t\to 0} \lambda(\theta^*, \phi^*, t) \neq 0$. It follows that there is no first time t_0 such that $y(t) \to d_{\text{sf}}$, and since $(\lambda(\theta, \phi, t) + d_{\text{sf}}) \geq y(t)$ and $d_{\text{sf}} > 0$, $\lambda(\theta, \phi, t) > 0$, the result is proved. ■

For moving obstacles, it is clear that collisions are inevitable in the case of the obstacle moving faster than vehicle's maximum speed, i.e.

$$\langle v_{\text{ob}}(t), \eta(\theta*, \phi*)\rangle > \|v_{\max}\| \tag{23}$$

where $v_{\text{ob}} \in \mathbf{R}^3$ is the velocity of the obstacle. Therefore, we have the following lemma.

Lemma 2. Given the same assumptions and conditions as in Lemma 1 and the obstacle speed assumption

$$\langle v_{\text{ob}}(t), \eta(\theta, \phi)\rangle \leq \|v_{\max}\|, \tag{24}$$

the proposed approach is also capable of avoiding moving obstacles in the environment, $\forall t > 0$ and $d_{\text{sf}} > 0$,

$$\lambda(\theta, \phi, t) > 0 \tag{25}$$

Proof. Given $y(t)$ has the same definition as in (13), an azimuth-elevation pair (θ^*, ϕ^*) still realizes (13) by (14). Considering the worst case scenario that $\lambda(\theta^*, \phi^*, t) < d_{\text{sf}}$ with the obstacle approaching speed of $\langle v_{\text{ob}}, \eta(\theta, \phi)\rangle \leq \|v_{\max}\|$, the following condition always holds according to (6),

$$\langle v(t), \eta(\theta, \phi)\rangle = \sqrt{\frac{2}{m}(E_{\text{p}} - E_{\max})}. \tag{26}$$

Combining (14), (26) and (24), one has

$$\begin{aligned} \sqrt{\frac{2}{m}(E_{\text{p}} - E_{\max})} &\leq \|v_{\max}\| \\ (\frac{4d_{\text{sf}}^2}{y(t)^2} - 1)\|v_{\max}\|^2 &\leq \|v_{\max}\|^2 \\ 2d_{\text{sf}}^2 &\leq y(t)^2 \\ \sqrt{2} d_{\text{sf}} &\leq y(t) \end{aligned} \tag{27}$$

Replacing $y(t)$ in (27) with (14) yields

$$\begin{aligned} \sqrt{2} d_{\text{sf}} &\leq \lambda(\theta^*, \phi^*, t) + d_{\text{sf}} \\ (\sqrt{2} - 1) d_{\text{sf}} &\leq \lambda(\theta^*, \phi^*, t) \end{aligned} \tag{28}$$

Therefore, $\forall t > 0$, given $d_{\text{sf}} > 0$, the inequality (28) implies that $\lambda(\theta, \phi, t) > 0$. The result is proved. ■

4. ENERGY BASED DYNAMIC KINESTHETIC BOUNDARY

The dynamic kinesthetic boundary (DKB) (Hou and Mahony [2013]) provides human operator with the environmental information by directly rendering spatial haptic cues in the master joystick workspace, and modulates the velocity set point to the slave robot to achieve obstacle avoidance. Considering the similarity between the proposed approach and DKB that both approaches modulate velocity set point to the slave robot based on the velocity upper bounds for obstacle avoidance, an energy based dynamic kinesthetic boundary (E-DKB) is proposed.

The E-DKB ${}^{\text{E}}\beta$ is defined by

$${}^{\text{E}}\beta(\theta, \phi, t) = \begin{cases} k_{\text{s}} \sqrt{1 - (\frac{2d_{sf}}{\lambda(\theta, \phi, t) + d_{sf}})^2} \|v_{\max}\|, \\ \qquad\qquad if\ E_{max} \geqslant E_p \\ -k_{\text{s}} \sqrt{(\frac{2d_{sf}}{\lambda(\theta, \phi, t) + d_{sf}})^2 - 1} \|v_{\max}\|, \\ \qquad\qquad if\ E_{max} < E_p \end{cases} \tag{29}$$

where k_{s} denotes the scaling factor that maps the slave velocity to the master displacement. The position reference

$\xi_{\text{ref}} \in \mathbf{R}^3$ for rendering the boundary in joystick workspace is given by

$$\xi_{\text{ref}}(t) = \begin{cases} k_{\text{s}} v(\theta,\phi,t), & \text{if } k_{\text{s}}\|v(\theta,\phi,t)\| \leq {}^{\text{E}}\beta(\theta,\phi,t) \\ {}^{\text{E}}\beta(\theta,\phi,t)\eta(\theta,\phi) & \text{if } k_{\text{s}}\|v(\theta,\phi,t)\| > {}^{\text{E}}\beta(\theta,\phi,t) \end{cases} \tag{30}$$

For the obstacle avoidance, the velocity set point to the slave vehicle is modulated by Algorithm 1 in admittance haptic joystick; for impedance haptic joystick, virtual surface rendering algorithms are needed (Zilles and Salisbury [1995]) and the algorithm becomes active only when penetration happens at the boundary, otherwise $\min_{v^*_{\text{ref}}}\{\hat{E}_{\text{k}}, E_{\text{d}}\} = E_{\text{d}}$ always holds and the velocity set point from user input can be used for regulating slave robot's velocity directly.

5. SIMULATION AND EXPERIMENT

In this section, we present simulation results for both static and dynamic obstacles to demonstrate the performance of the proposed energy based obstacle avoidance. Experiment data from an experimental platform was obtained and further demonstrates the performance of the proposed approach in avoidance collisions.

5.1 Simulation

Provided the maximum velocity of the salve robot $\|v_{\max}\| = 0.5m/s$ and the safety distance $d_{\text{sf}} = 0.8m$, the slave robot was deployed at $(3, 0)$, three meters away from an obstacle at $(0, 0)$. A constant maximum velocity set point was applied during the simulation, i.e. $v_{\text{ref}} = v_{\max}$.

Static obstacles In Fig. 2, as the vehicle approached the wall, the permissible kinetic energy towards the wall kept decreasing and reduced to zero at the safety distance d_{sf}, which brought the slave robot to still without passing the safety distance d_{sf}. The energy exchanges between vehicle's potential energy and kinetic energy can be easily observed in the bottom plot.

Moving obstacles In this set of simulations, the obstacle started to move towards the robot at two difference speeds, i.e. a slow speed $0.2m/s$ and vehicle's maximum speed $0.5m/s$, after the vehicle reaching d_{sf}. Figure 3 presents the result of the simulation that the obstacle approaches at $0.2m/s$ towards the slave. As the obstacle started moving, the distance between robot and obstacles dropped below d_{sf}, and excessive potential energy in the slave system drove the vehicle away from the obstacles; when the vehicle traveled at the same speed as the obstacle, the distance between robot and obstacle stopped decreasing. There was no collision during the simulation. When obstacle moved at vehicle's maximum speed, the result in Fig. 4 suggests that, with proper parameter settings, the proposed obstacle avoidance algorithm is capable of avoiding moving obstacles even if the obstacles are moving as faster as the slave robot travels.

5.2 Experimental Setup

The experiment was carried out on an aerial robot platform equipped with laser scanner that provides 270 degree FOV for detecting obstacles controlled a customized built 3D admittance haptic joystick. The experiment environment is covered by a VICON tracking system and vehicle's velocity is controlled by velocity controller using velocity estimation from VICON data (Hou et al. [2013]).

The experiment was set up the same as the simulation, i.e.$d_{\text{sf}} = 0.8m$, $\|v_{\max}\| = 0.5m/s$. The pilot deliberately commanded the vehicle to approach a static obstacle. It is expected that, the proposed energy based obstacle avoidance algorithm will prevent vehicle from possible collision with static obstacles. Due to the safety concern, the moving obstacle experiment can not be conducted.

5.3 Experiment result

Experimental data of approaching a static obstacle is shown in Fig. 5. User deliberately commanded the quadrotor robot to approach the obstacle by keeping giving velocity set point towards the obstacle. In the zoomed part of Fig. 5, the performance of the proposed algorithm can be clearly demonstrated that, initially the user input and actual set point agreed until the permissible kinetic energy $\hat{E}_{\text{k}}$ was not sufficient to achieve desired kinetic energy E_{d}, then the proposed approach modulated the reference input according to $\hat{E}_{\text{k}}$, and stopped the vehicle. In the bottom left figure, the set point becoming negative indicates vehicle's passing the safety distance due to the performance of the velocity controller of slave robot, but the vehicle was driven back to the safety distance [1]. No collision happened during the experiment.

6. CONCLUSION

In this paper, we propose an energy based obstacle avoidance approach with its implementation in dynamic kinesthetic boundary for haptic teleoperation of VTOL aerial robots. This approach introduces the potential energy into the passive teleoperation framework to modulate the velocity set point to vehicle's velocity controller by comparing the user desired and permissible kinetic energy and the environment potential energy to achieve obstacle avoidance. The E-DKB also extends the research outcomes to exploit the spatial haptic cues for providing human operator with better perception and awareness of the remote environment. Analysis, simulation and experiment results provide strong support to our claims of the guaranteed obstacle avoidance performance of the novel approach.

REFERENCES

Boschloo, H., Lam, T., Mulder, M., and van Paassen, M. (2004). Collision avoidance for a remotely-operated helicopter using haptic feedback. In *Proc. 2004 IEEE Int. Conf. Syst. Man Cybern.*, volume 1, 229–235.

Brandt, A. and Colton, M.B. (2010). Haptic collision avoidance for a remotely operated quadrotor uav in indoor environments. In *Proc. 2010 IEEE Int. Conf. Syst. Man Cybern.*, 2724 –2731.

Diolaiti, N. and Melchiorri, C. (2002). Teleoperation of a mobile robot through haptic feedback. In *Proc. 2002 IEEE Int. Workshop Haptic Virtual Environments and Their Applications*, 67 – 72.

[1] The performance of the slave's velocity controller should be taken into account when designing the safety distance d_{sf}.

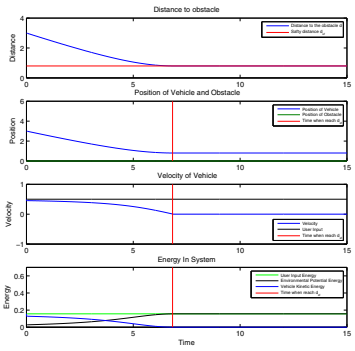

Fig. 2. Approaching a static obstacle

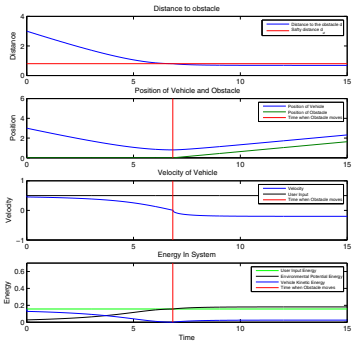

Fig. 3. Approaching a moving obstacle at 0.2m/s

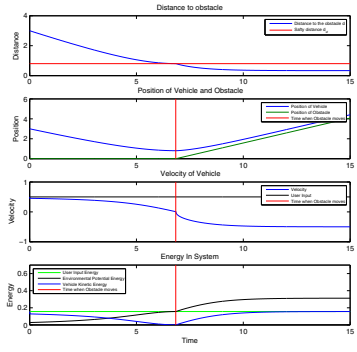

Fig. 4. Approaching a moving obstacle at 0.5m/s

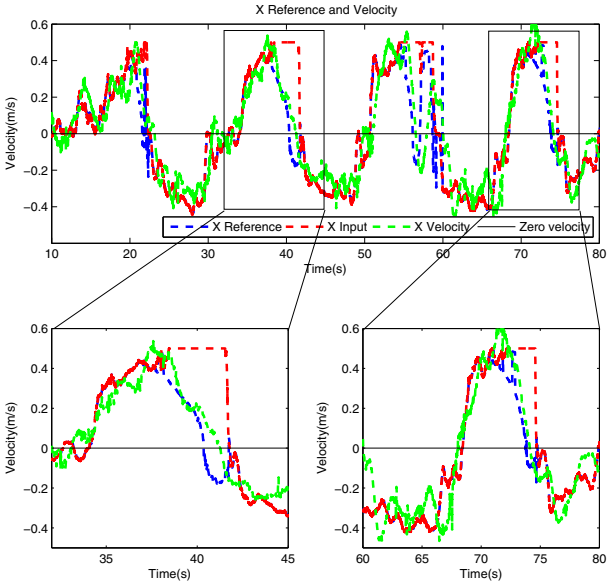

Fig. 5. Result of static obstacle experiment

Farkhatdinov, I. and Ryu, J.H. (2007). Hybrid position-position and position-speed command strategy for the bilateral teleoperation of a mobile robot. In *Proc. 2007 Int. Conf. Control, Autom. Syst.*, 2442 –2447.

Hong, S.G., Lee, J.J., and Kim, S. (1999). Generating artificial force for feedback control of teleoperated mobile robots. In *Proc. 1999 IEEE/RSJ Int. Conf. Intell. Robots Syst.*, volume 3, 1721–1726 vol.3.

Hou, X. and Mahony, R. (2013). Dynamic kinesthetic boundary for haptic teleoperation of aerial robotic vehicles. In *Proc. 2013 IEEE/RSJ Int. Conf. Intell. Robots Syst.*, 4549–4950.

Hou, X., Mahony, R., and Schill, F. (2013). Representation of vehicle dynamics in haptic teleoperation of aerial robots. In *Proc. 2013 IEEE Int. Conf. Robot. and Autom.*, 1447–1483.

Kim, K., Chung, W.K., and Suh, I.H. (2006). Accurate force reflection for kinematically dissimilar bilateral teleoperation systems using instantaneous restriction space. In *Proc. 2006 IEEE Int. Conf. Robot. and Autom.*, 3257 –3262.

Krogh, B. (1984). A generalized potential field approach to obstacle avoidance control. In *Proc. conf. Robot. Res.: The Next Five Years and Beyond*, 1–5.

Lam, T.M., Boschloo, H.W., Mulder, M., and van Paassen, M.M. (2009). Artificial force field for haptic feedback in uav teleoperation. *IEEE Trans. Syst. Man Cybern. A., st. Humans*, 39(6), 1316 –1330.

Lam, T.M., Mulder, M., and van Paassen, M.M. (2007). Collision avoidance in uav tele-operation with time delay. In *Proc. 2007 IEEE Int. Conf. Syst. Man Cybern.*, 997 –1002.

Lee, D. and Huang, K. (2010). Passive-set-position-modulation framework for interactive robotic systems. *IEEE Trans. on Robot.*, 26(2), 354 –369.

Lee, D., Martinez-Palafox, O., and Spong, M. (2006). Bilateral teleoperation of a wheeled mobile robot over delayed communication network. In *Proc. 2010 IEEE Int. Conf. Robot. and Autom*, 3298–3303.

Lee, S., Sukhatme, G.S., Kim, G.J., and Park, C.M. (2002). Haptic control of a mobile robot: a user study. In *Proc. 2002 IEEE/RSJ Int. Conf. Intell. Robots Syst.*, volume 3, 2867 – 2874.

Mahony, R., Schill, F., Corke, P., and Oh, Y.S. (2009). A new framework for force feedback teleoperation of robotic vehicles based on optical flow. In *Proc. 2009 IEEE Int. Conf. Robot. and Autom.*, 1079 –1085.

Mersha, A.Y., Ruesch, A., Stramigioli, S., and Carloni, R. (2012). A contribution to haptic teleoperation of aerial vehicles. In *Proc. 2012 IEEE/RSJ Int. Conf. Intell. Robots Syst.*, 3041–3042.

Omari, S., Hua, M., Ducard, G., and Hamel, T. (2013). Bilateral haptic teleoperation of vtol uavs. In *Proc. 2013 IEEE Int. Conf. Robot. and Autom.*, 2385–2391.

Schill, F., Mahony, R., Corke, P., and Cole, L. (2008). Virtual force feedback teleoperation of the insectbot using optical flow. In *Proc. 2008 Australasian Conf. Robot. Autom.* Canberra, Australia.

Stramigioli, S., Mahony, R., and Corke, P. (2010). A novel approach to haptic teleoperation of aerial robot vehicles. In *Proc. 2010 IEEE Int. Conf. Robot. and Autom.*

Zilles, C.B. and Salisbury, J.K. (1995). A constraint-based god-object method for haptic display. In *Proc. 1995 IEEE/RSJ Int. Conf. Intell. Robots Syst.*, volume 3, 146 –151 vol.3.

Zuo, Z. and Lee, D. (2010). Haptic tele-driving of a wheeled mobile robot over the internet: A pspm approach. In *Proc. 2010 IEEE Int. Conf. Decis. and Cont.*, 3614–3619.